Dynamics of topological defects in a spiral: a scenario for the spin-glass phase of cuprates

V. Juricic¹, A. O. Caldeira², and C. Morais Smith¹

¹Département de Physique, Université de Fribourg, Pérolles, CH-1700 Fribourg, Switzerland.

² Instituto de Física Gleb Wataghin, Universidade Estadual de Campinas, 13083-970, Campinas, SP, Brazil

We propose that the dissipative dynamics of topological defects in a spiral state is responsible for the transport properties in the spin-glass phase of cuprates. Using the collective-coordinate method, we show that topological defects are coupled to a bath of magnetic excitations. By integrating out the bath degrees of freedom, we show that the dynamical properties of the topological defects are dissipative. The calculated damping matrix is related to the in-plane resistivity, which exhibits an anisotropy and temperature dependence in agreement with available experimental data.

PACS numbers:

The discovery of four static incommensurate (IC) charge and spin peaks by neutron scattering experiments in Nd-doped $La_{2-x}Sr_xCuO_4$ (LSCO) [1] confirmed the proposal that in these materials the holes form vertical/horizontal charge stripes [2], breaking the paradigm of homogeneous charge distribution. Moreover, the observation of IC dynamical spin correlations in superconducting LSCO (x > 0.05) at the same wave vectors as observed in the Nd-doped compounds [3] placed the stripe picture on a more solid footing and raised further questions concerning the coexistence of magnetism and superconductivity. Later, two IC elastic magnetic peaks have been observed within the spin-glass (SG) phase of LSCO (0.02 < x < 0.05) [4], and their interpretation in terms of diagonal stripe formation appeared to be rather natural, given that the value of the magnetic IC follows the same linear dependence on doping as observed within the superconducting regime [4]. However, no charge order has ever been measured in the SG regime, and the picture of well-ordered stripes, very far apart from each other due to the very low doping concentration, seems guite improbable because disorder and frustration effects, which act to destabilize the stripes, are expected to dominate in this phase.

A different explanation of the two IC peaks in the SG phase is that these may arise from the formation of a spiral magnetic order which breaks the translational symmetry in the spin but not in the charge sector [5]. In this model, the randomly distributed holes act as frustration centers for the underlying antiferromagnetic background, generating a dipole moment. A fraction of these dipoles may order ferromagnetically, while the others may remain disordered. If the number of ordered dipoles increases linearly with the doping concentration, which would appear plausible, this model describes completely the experimentally observed linear variation of the IC magnetic wave vector with doping [4], without invoking charge ordering [5].

Recently, transport properties along both diagonaldirections in the Cu lattice have been investigated in high-quality, detwinned LSCO samples, and a rather strong anisotropy was detected [6]. However, this experiment provides no definitive evidence in favor of the stripe picture, because similar anisotropic behavior would be expected for transport parallel or perpendicular to the spiral axis.

In this paper we investigate the formation of topological defects in the spiral state which couple to excitations of the magnetic environment and diffuse across the system. We assume that the charge carriers are attached to these defects and therefore the description of defect dynamics corresponds ultimately to the electrical transport properties of cuprates in the SG phase. We evaluate the damping matrix, which is related to the kink mobility, and show that its behavior at low and high temperatures follows the experimentally observed temperature (T) dependence of the in-plane resistivity. In addition, we account for the anisotropy in the spin-wave velocity in the directions parallel and perpendicular to the spiral axis, and find that, in agreement with experiments, it leads to an anisotropy in the resistivity.

Topological defects in the spiral state originate from the chiral degeneracy of the spiral [7]. Their description is provided by the elements $\exp(im^a\sigma^a\Psi/2)$ of the fundamental representation of the SU(2) group (the generators are the Pauli matrices σ^a). The parameters $\mathbf{m}\Psi$ are related to the local spin, where \mathbf{m} is a constant unit vector and Ψ is a scalar field [8]. The action describing free topological defects in the spiral state is [5]

$$S_f = \frac{J}{16} \int dt dx_{\parallel} dx_{\perp} [(\partial_t \Psi)^2 - c_{\perp}^2 (\partial_{x_{\perp}} \Psi)^2 - c_{\parallel}^2 (\partial_{x_{\parallel}} \Psi)^2].$$

J is the antiferromagnetic exchange and c_{\perp} , c_{\parallel} are the spin wave velocities perpendicular and parallel to the spiral, with $(c_{\parallel}/c_{\perp})^2 = \cos{(Qa)}$ [5]. Here a is the lattice constant and Q is the IC magnetic wave vector observed by neutron scattering. This action may be mapped to an isotropic form by introducing the coordinates $\mathbf{r} = (x,y)$ with $x = \sqrt{c_{\parallel}/c_{\perp}}x_{\perp}$, $y = \sqrt{c_{\perp}/c_{\parallel}}x_{\parallel}$, and the corresponding equation of motion has the form

$$(\partial_t^2 - c^2 \nabla^2) \Psi(t, \mathbf{r}) = 0, \tag{1}$$

where $c = \sqrt{c_{\perp} c_{\parallel}}$ is the isotropic spin-wave velocity. We begin by considering the static limit, where Eq. (1) becomes the Laplace equation $\nabla^2 \Psi(\mathbf{r}) = 0$. A non-trivial solution $\Psi_{1k}(\mathbf{r},\mathbf{R}) = \arctan(y-Y)/(x-X)$ has the form of a kink centered at $\mathbf{R} = (X, Y)$, and the corresponding energy $E \propto \ln L/a$ diverges with the system size L. Unbound, free topological defects cannot therefore exist at low temperatures. However, the twokink solution $\Psi_{2k} = \Psi_{1k}(\mathbf{r}, \mathbf{R_1}) - \Psi_{1k}(\mathbf{r}, \mathbf{R_2})$, which describes a bound pair of topological defects (kink and antikink), centered respectively at \mathbf{R}_1 and \mathbf{R}_2 , has a finite energy $E(\Psi_{2k}) \propto \ln(d/a)$, where $d = |\mathbf{R}_1 - \mathbf{R}_2|$ is the modulus of the kink relative coordinate which we take as a constant. It is convenient to express the twokink solution in terms of its center of mass and relative coordinate, which, up to an irrelevant constant, yields $\Psi_{2k}(\mathbf{r}) = \arctan\{[(\mathbf{r} - \mathbf{R}) \times \mathbf{d}]_z/[(\mathbf{r} - \mathbf{R})^2 - d^2/4]\}.$ The complete action of the system includes the interaction among topological defects,

$$S = \frac{J}{16} \int dt d^2r \left[(\partial_t \Psi)^2 - c^2 (\nabla \Psi)^2 + g(\Psi \nabla \Psi)^2 \right], \quad (2)$$

where g is a small coupling constant. The interaction in (2) was chosen to be relevant in the renormalization group sense as well as to produce a long range effective potential for the magnons. We will apply the collective coordinate method [9] to study the dynamics of a bound pair of topological defects in a spiral phase. We first expand the dynamical solution around the static one,

$$\Psi(\mathbf{r} - \mathbf{R}, t) = \Psi_{2k}(\mathbf{r} - \mathbf{R}) + \sum_{n=0}^{\infty} q_n(t) \eta_n(\mathbf{r} - \mathbf{R}), \quad (3)$$

where η_n are the eigenfunctions of the second variational derivative of the action

$$[-c^2\nabla^2 + V(\mathbf{r})]\eta_n = \omega_n^2 \eta_n. \tag{4}$$

Here, the potential $V(\mathbf{r}) = g\nabla\Psi_{2k}(\mathbf{r})\nabla\Psi_{2k}(\mathbf{r})$ describes the scattering of the excitations around the two-kink configuration. After expansion in the small parameter $d \ll r$, one obtains

$$V(r) = -\frac{gd^2}{2r^4} \equiv -\frac{\alpha(d)}{r^4}.$$
 (5)

The solutions of Eq. (4) have the form $\eta_{mn} \propto [H_m^{(1)}(k_{mn}r) + e^{-2i\delta_m}H_m^{(2)}(k_{mn}r)] e^{im\theta}$, where $H_m^{(1,2)}$ are Henkel functions of the first and second kinds, δ_m represents a phase shift for the mode m, and θ is a polar angle. The excitation with frequency ω_{mn} has the dispersion $\omega_{mn} = c|\mathbf{k}_{mn}|$. The Goldstone modes $\nabla \Psi_{2k} \equiv (\partial_x \Psi_{2k}, \partial_y \Psi_{2k})$ are associated with the continuous translational symmetry of the model. In order to avoid the technical problems related to the presence of zero-frequency modes, the center of the kink \mathbf{R} is promoted to a dynamical variable, giving

$$\Psi(\mathbf{r},t) = \Psi_{2k}(\mathbf{r} - \mathbf{R}(t)) + \sum_{mn} q_{mn}(t)\eta_{mn}(\mathbf{r} - \mathbf{R}(t)).$$
 (6)

A lengthy but straightforward procedure [9] leads to the effective action describing a topological defect interacting with the excitations of its magnetic environment,

$$H = \frac{1}{2M} (\mathbf{P} - \mathbf{P}_s)^2 + \frac{1}{2} \sum_{mn} (p_{mn}^2 + \omega_{mn}^2 q_{mn}^2), \quad (7)$$

where M is the kink mass, \mathbf{P} and p_{mn} are respectively the momentum conjugate to \mathbf{R} and to the coordinate q_{mn} of the excitation with frequency ω_{mn} , and $\mathbf{P}_s = \sum_{mn,kl} p_{mn} \mathbf{G}_{mn,kl} q_{kl}$. The constants $\mathbf{G}_{mn,kl}$ are related to the eigenfunctions η by $\mathbf{G}_{mn,kl} = \int d^2r \eta_{kl} \nabla \eta_{mn}$. The classical Hamiltonian (7) is quantized by introducing creation and annihilation operators a_{mn}^{\dagger} and a_{mn} , yielding

$$\hat{H} = \frac{1}{2M}(\hat{\mathbf{P}} - \hat{\mathbf{P}}_s)^2 + \sum_{mn} \hbar \omega_{mn} \, a_{mn}^{\dagger} a_{mn}, \qquad (8)$$

with the operator

$$\hat{\mathbf{P}}_{s} = \sum_{mn,kl} \left[-\mathbf{D}_{mn,kl}^{(+)} a_{mn}^{\dagger} a_{kl} + \mathbf{D}_{mn,kl}^{(-)} a_{mn} a_{kl} + H.c. \right].$$

The coupling constants are given by $\mathbf{D}_{mn,kl}^{(\pm)} = \mathcal{G}_{mn,kl}(\omega_{mn} \pm \omega_{kl})$, where $\mathcal{G}_{mn,kl} = \mathbf{G}_{mn,kl}/4i\sqrt{\omega_{mn}\omega_{kl}}$. The terms proportional to $\mathbf{D}^{(+)}$ commute with the total number of excitations, and therefore describe elastic scattering, whereas the $\mathbf{D}^{(-)}$ terms describe processes with creation and annihilation of excitations. At quadratic order in a_{mn}^{\dagger} , a_{mn} we obtain

$$\hat{H} = \frac{\hbar \hat{\mathbf{P}}}{M} \sum_{mn,kl} \left[\mathbf{D}_{mn,kl}^{(+)} a_{mn}^{\dagger} a_{kl} - \mathbf{D}_{mn,kl}^{(-)} a_{mn} a_{kl} + H.c. \right]$$

$$+ \frac{\hat{\mathbf{P}}^{2}}{2M} + \sum_{mn} \hbar \omega_{mn} a_{mn}^{\dagger} a_{mn}.$$

$$(9)$$

Our aim is to investigate, in the low-energy sector, the effective dynamics of kinks in the presence of an excitation bath. Because in this sector the effective dynamics of the kinks are influenced primarily by elastic processes, we neglect in what follows all inelastic contributions $(\mathbf{D}^{(-)} = 0 \text{ and } \mathbf{D}^{(+)} \equiv \mathbf{D})$. We compute the reduced density matrix of the kink by integrating out the degrees of freedom of the bath [9], for which we employ the Feynman-Vernon path-integral formalism. The evolution of the density matrix for the full system is described by $\hat{\rho}(t) = \exp(-i\hat{H}t/\hbar)\hat{\rho}(0)\exp(i\hat{H}t/\hbar)$. For the sake of simplicity, we use the factorizable initial condition $\hat{\rho}(0) = \hat{\rho}_k(0)\,\hat{\rho}_b(0)$, where ρ_k and $\hat{\rho}_b$ represent, respectively, the initial kink and bath density matrices. This condition implies that the kink and the excitations do not interact at t = 0. The bath degrees of freedom are supposed to be initially in thermal equilibrium, $\hat{\rho}_b(0) =$ $e^{-\beta \hat{H}_b}/Tr[e^{-\beta \hat{H}_b}]$, where $\hat{H}_b \equiv \sum_{mn} \hbar \omega_{mn} a_{mn}^{\dagger} a_{mn}$ and

 $\beta \equiv \hbar/k_BT$. After evaluating the trace over these, we obtain the reduced density-matrix operator for the kink

$$\hat{\tilde{\rho}}(\mathbf{x}, \mathbf{y}, t) = \int \int d\mathbf{x}' d\mathbf{y}' J(\mathbf{x}, \mathbf{y}, t; \mathbf{x}', \mathbf{y}', 0) \hat{\rho}_k(\mathbf{x}', \mathbf{y}', 0),$$

where the superpropagator J has the form

$$J = \int_{\mathbf{x}'}^{\mathbf{x}} \mathcal{D}\mathbf{x} \int_{\mathbf{y}'}^{\mathbf{y}} \mathcal{D}\mathbf{y} e^{\frac{i}{\hbar}[S_0[\mathbf{x}] - S_0[\mathbf{y}]]} \mathcal{F}[\mathbf{x}, \mathbf{y}]. \tag{10}$$

 $S_0[\mathbf{x}] = \int_0^t dt'(M/2)\dot{\mathbf{x}}^2$ is the action associated with the free motion of the kink and $\mathcal{F}[\mathbf{x}, \mathbf{y}] = [\det(1 - N\Gamma)]^{-1}$ is the influence functional, which describes the effect of the excitations on the dynamics of the topological defect. The boson occupation number is $N_{mn} = (e^{\beta \omega_{mn}} - 1)^{-1}$ and the matrix Γ is given by

$$\Gamma = W^{T}(\mathbf{x}, t) + W^{*}(\mathbf{y}, t) + \frac{1}{2}W^{T}(\mathbf{x}, t)W^{*}(\mathbf{y}, t),$$

with the functional W determined from the solution of

$$\dot{W}[\mathbf{x}, \tau] = W^{0}[\mathbf{x}, \tau] + W^{0}(\mathbf{x}, \tau)W(\mathbf{x}, \tau), \tag{11}$$

where $W_{mn,kl}^0(\mathbf{x},\tau) = -2i\dot{\mathbf{x}}\mathbf{D}_{mn,kl}e^{i(\omega_{mn}-\omega_{kl})\tau}$.

Calculation of the influence functional requires the solution of Eq. (11), which is possible up to any order within the Born approximation. Because we consider here only the low-energy sector of the theory, a second-order iteration will be sufficient for our purposes. Defining the center of mass and relative coordinates $\mathbf{v} = (\mathbf{x} + \mathbf{y})/2, \mathbf{u} = \mathbf{x} - \mathbf{y}$, one obtains the influence functional

$$\mathcal{F}[\mathbf{x}, \mathbf{y}] = \exp[i\Phi] \exp[\tilde{\Phi}], \tag{12}$$

where

$$\begin{split} \Phi \; &= \; 2 \sum_{\mu,\nu=1}^2 \int_0^t dt' \int_0^{t'} dt'' \epsilon^{\mu\nu} (t'-t'') \dot{u}^\mu (t') \dot{v}^\nu (t''), \\ \tilde{\Phi} \; &= \; \sum_{\mu\nu} \int_0^t dt' \int_0^{t'} dt'' \tilde{\epsilon}^{\mu\nu} (t'-t'') \dot{u}^\mu (t') \dot{u}^\nu (t''), \\ \epsilon^{\mu\nu} (t) \; &= \; 4 \sum_{mn,kl \neq 0} N_{mn} D^\mu_{mn,kl} D^\nu_{mn,kl} \sin{(\omega_{mn} - \omega_{kl})t}, \\ \tilde{\epsilon}^{\mu\nu} (t) \; &= \; 4 \sum_{mn,kl \neq 0} N_{mn} D^\mu_{mn,kl} D^\nu_{mn,kl} \cos{(\omega_{mn} - \omega_{kl})t}. \end{split}$$

The effective action which describes the motion of the kinks in the presence of excitations may then be obtained by inserting Eq. (12) into the superpropagator (10). We find that $S_{eff} = S_0[\mathbf{x}] - S_0[\mathbf{y}] + \hbar \Phi$ and the corresponding equations of motion are

$$\ddot{v}^{\mu}(\tau) + \sum_{\nu} \int_{0}^{\tau} dt' \gamma^{\mu\nu} (\tau - t') \, \dot{v}^{\nu}(t') = 0,$$

$$\ddot{u}^{\mu}(\tau) - \sum_{\nu} \int_{\tau}^{t} dt' \gamma^{\mu\nu} (t' - \tau) \dot{u}^{\nu}(t') = 0, \quad (13)$$

where $\gamma^{\mu\nu}(t)=(2\hbar/M)\dot{\epsilon}^{\mu\nu}(t)$. Eqs. (13) indicate that the motion of the kink is damped. The matrix γ represents a generalization of the damping coefficient, and is the inverse of the kink mobility μ^{-1} . The decaying part $\exp[\tilde{\Phi}]$ of the influence functional is related to the diffusive properties of the kink, with the diffusion matrix $D^{\mu\nu}(t)=\hbar\tilde{\epsilon}^{\mu\nu}(t)$. Evaluation of the diffusion is analogous to that of the damping matrix, and at low T the two parameters are related by the fluctuation-dissipation theorem. Because we wish to calculate the resistivity $\rho\propto\mu^{-1}\propto\gamma$, we will concentrate on γ only. We first introduce the scattering function

$$S^{\mu\nu}(\omega,\omega') = \sum_{mn,kl} G^{\mu}_{mn,kl} G^{\nu}_{mn,kl} \delta(\omega - \omega_{mn}) \delta(\omega' - \omega_{kl}).$$

Because the model we study is isotropic, the damping matrix is diagonal $\gamma^{\mu\nu}(t) = \gamma(t)\delta^{\mu\nu}$, and $\gamma(t)$ is obtained directly from the first derivative $\dot{\epsilon}(t)$,

$$\gamma(t) = \frac{\hbar}{8M} \int_{-\infty}^{\infty} d\omega \int_{-\infty}^{\infty} d\omega' [N(\omega) - N(\omega')] (\omega^2 - \omega'^2) \times \frac{(\omega + \omega')}{\omega \omega'} S(\omega, \omega') \cos [(\omega - \omega')t],$$

where $S(\omega, \omega')$ is the diagonal part of the scattering function. After introducing the substitution $\xi = (\omega + \omega')/2, \zeta = \omega - \omega'$, and considering only processes for which $\zeta \ll 1$, we find that $\gamma(t) = \bar{\gamma}(T)\delta(t)$ with

$$\bar{\gamma}(T) = -\frac{\hbar}{2M} \int_0^\infty d\xi \varphi(\xi) \frac{\partial N(\xi)}{\partial \xi},\tag{14}$$

where

$$\varphi = 4\pi^2 \left[\frac{1}{2} (1 - \sin 2\delta_2) + \sum_{m=2}^{\infty} \frac{\pi^2 (\kappa_{m+1} - \kappa_m)^2}{A_m} \right],$$

and $A_m = 1 + 2(\Delta_m + \Delta_{m+1})$. The phase shifts δ_m are given by $\delta_m = \arctan[\pi \kappa_m/(1 + \Delta_m)]$, the matrix element $\kappa_m = -\langle m|V|m\rangle = F_m\omega^2$, and $\Delta_m = -i\mathcal{P}\int_0^\infty \kappa_m (k^2 - x^2)^{-1}xdx = \pi F_m\omega^2$ for the potential (5) with $F_m = \pi\alpha/2c^2m(m^2-1)$. We note that $\delta_1 = \pi/4$ because $F_1 \to \infty$, and that because the coefficients κ_m are small, we have neglected all the quadratic terms in the evaluation of A_m .

Let us now calculate the asymptotic temperature dependence of the damping coefficient. At high T we obtain

$$\bar{\gamma}(T) = \frac{k_B T}{2M} \int_0^\infty d\xi \frac{\varphi(\xi)}{\xi^2} \propto T.$$
 (15)

Because the resistivity ρ is proportional to the damping coefficient, this result implies that in the high-T limit ρ varies linearly with T, as observed experimentally.

In the low-T limit, the assumption $\beta \xi \gg 1$ in the generic expression for the damping coefficient (14) leads

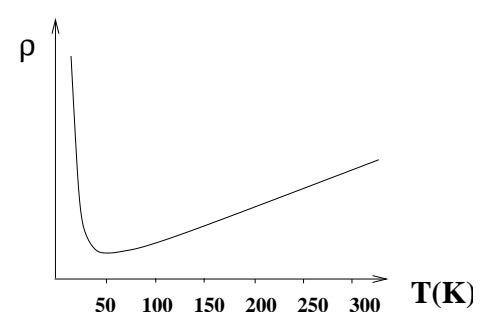


FIG. 1: In-plane resistivity in arbitrary units as a function of T, as given by Eqs. (15) and (16). Notice the linear dependence at high-T and the upturn at low-T, in agreement with experimental observations.

to an integral, whose analytical solution gives $\bar{\gamma}(T) = (\pi^4 \hbar/M) \sum_{m=1}^{\infty} \bar{\gamma}_m(T)$, where

$$\bar{\gamma}_{m}(T) = \frac{2(\tilde{F}_{m+1} - \tilde{F}_{m})^{2}}{\beta^{2}\sigma_{m}^{2}} \left\{ \left(2 - \frac{\beta^{2}}{\sigma_{m}^{2}}\right) (1 - \delta_{m,1}) + \frac{\beta^{3}}{\sigma_{m}^{3}} \left[1 + (\pi^{2} - 1)\delta_{m,1}\right] \left[ci\left(\frac{\beta}{\sigma_{m}}\right)\sin\left(\frac{\beta}{\sigma_{m}}\right) - si\left(\frac{\beta}{\sigma_{m}}\right)\cos\left(\frac{\beta}{\sigma_{m}}\right)\right] \right\},$$
(16)

with $\tilde{F}_m = (1 - \delta_{m,1}) F_m$ and $\sigma_m = \sqrt{2\pi (\tilde{F}_m + \tilde{F}_{m+1})}$. In the low-energy sector of the theory, we may estimate that $F_m = \pi g d^2 / 4c^2 m (m^2 - 1)$. The coefficients with the lowest values of m are therefore the most important, and obey $\beta / \sigma_m \sim \hbar c / \sqrt{g} dk_B T$. Although the exact microscopic values of the parameters d, c, and g are not available, we nevertheless provide a crude estimate of these. Using that $\hbar c/a \sim 100 \text{meV}$ [10], $d \sim ax^{-1} \sim 50a$ (for x = 0.02) and $g \sim 0.3 \ll 1$, we obtain $\beta / \sigma_2 \sim 40 / T$. The evolution of $\bar{\gamma}(T)$ as given by Eqs. (15) and (16) is shown in Fig. 1. We note the qualitative overall agreement with resistivity measurements in the SG phase: a linear T dependence at high T, with an upturn at lower T.

In order to provide a more detailed comparison with the available experimental data, we reexpress our results in the reference frame $(x_{\parallel}, x_{\perp})$ fixed to the spiral. Due to the anisotropy [4], the diagonal elements of the damping matrix $\bar{\gamma}^{\perp} \propto (D_{\perp})^2 \propto (G^{\perp})^2 \propto (c_{\parallel}/c_{\perp})\bar{\gamma}$, and similarly, $\bar{\gamma}^{\parallel} \propto (c_{\perp}/c_{\parallel})\bar{\gamma}$. As a consequence, the resistivity in the spiral direction is larger than that in the direction perpendicular to it, $\gamma_{\perp}/\gamma_{\parallel} = \rho_{\perp}/\rho_{\parallel} = (c_{\parallel}/c_{\perp})^2 = \cos{(Qa)} < 1$. This result is in agreement with transport measurements by Ando et al. [6], which found that below $T \sim 150 \mathrm{K}$ the resistivity along the a-axis in LSCO is smaller than along the b-axis (in orthorhombic coordinates). We note that the IC peaks observed in neutron scattering correspond to the b-direction, which coincides with the spiral axis because the breaking of

translational symmetry within the spiral picture has its origin in the spiral chirality (which can rotate clock- or counter-clockwise). Thus, $\rho_{\perp} \equiv \rho_a, \rho_{\parallel} \equiv \rho_b$ and $\rho_a < \rho_b$, as experimentally observed. This result demonstrates that the measured anisotropy in transport experiments in the SG phase does *not* provide evidence for the existence of diagonal stripes, but instead, is also the result expected within a more realistic, albeit more complex, model which does not need to appeal to charge order at such small doping concentrations.

In conclusion, we propose a description of the transport properties in the SG phase of cuprates based on the dissipative dynamics of topological defects in a spiral state. Using the collective-coordinate method, we derive the effective action of the topological defects, which are coupled to a bath of magnons. The scattering of magnons in the potential provided by the topological defects leads to a dissipative motion for these defects. The corresponding damping matrix is calculated, and is related to the in-plane resistivity. Its temperature dependence and anisotropic behavior are in agreement with the available experimental data, indicating that further investigations are required to distinguish between spiral spin states and diagonal stripes in the SG phase of cuprates.

We acknowledge fruitful discussions with N. Hasselmann, B. Normand, A. H. Castro Neto, V. Gritsev, and L. Benfatto. One of us (AOC) wishes to thank Fundação de Amparo à Pesquisa no Estado de São Paulo (FAPESP) and Conselho Nacional de Desenvolvimento Científico e Tecnológico (CNPq) for their financial aid. This work was supported by the Swiss National Foundation for Scientific Research under grant No. 620-62868.00.

- [1] J. M. Tranquada et al., Nature (London) **375**, 561 (1995).
- [2] J. Zaanen and O. Gunnarsson, Phys. Rev. B 40, 7391 (1989).
- [3] K. Yamada et al., Phys. Rev. B 57, 6165 (1998).
- [4] S. Wakimoto et al., Phys. Rev. B 60, R769 (1999); ibid.
 61, 3699 (2000); M. Matsuda et al., ibid. 62, 9148 (2000);
 M. Fujita et al., ibid. 61, 3699 (2000); ibid. 65, 064505 (2002).
- [5] N. Hasselmann, A. H. Castro Neto, and C. Morais Smith, Europhys. Lett. 56, 870 (2001); *ibid.*, preprint.
- [6] Y. Ando et al., Phys. Rev. Lett. 87, 017001 (2001); ibid. 88, 137005 (2002).
- [7] H. Kawamura, J. Phys. Condens. Matter 10, 4707 (1998).
- 8 M. Wintel, H. U. Everts, and W. Apel, Europhys. Lett. **25**, 711 (1994); *ibid.* Phys. Rev. B **52**, 13480 (1995).
- [9] A. H. Castro Neto and A. O. Caldeira, Phys. Rev. Lett.
 67, 1960 (1991); *ibid.* Phys. Rev. B 46, 8858 (1992); *ibid.* Phys. Rev. E 48, 4037 (1993); A. V. Ferrer and A. O. Caldeira, Phys. Rev. B 61, 2755 (2000).
- [10] M. Vojta, C. Buragohain, and S. Sachdev, Phys. Rev. B 61, 15152 (2000).